Spectrochimica Acta Part A: Molecular and Biomolecular Spectroscopy 120 (2014) 314–322

Contents lists available at ScienceDirect

Spectrochimica Acta Part A: Molecular and Biomolecular Spectroscopy

journal homepage: www.elsevier.com/locate/saa

Synthesis and spectral characterization of hydrazone derivative of furfural using experimental and DFT methods

N. Ramesh Babu [a], S. Subashchandrabose [b], M. Syed Ali Padusha [c], H. Saleem [d,*], Y. Erdoğdu [e]

[a] Dept. of Physics, M.I.E.T. Engineering College, Trichy, Tamil Nadu 620007, India
[b] Dept. of Physics, M.A.R College of Engineering & Technology, Trichy, Tamil Nadu 621316, India
[c] PG and Research Dept. of Chemistry, Jamal Mohamad College (Autonomous), Tiruchirapalli, Tamil Nadu 620020, India
[d] Dept. of Physics, Annamalai University, Annamalai Nagar, Tamil Nadu 608 002, India
[e] Dept. of Physics, Ahi Evran University, Kirsehir 40040, Turkey

HIGHLIGHTS

- Total energy distribution analysis.
- Natural bond orbital analysis.
- Non-linear optical behavior hydrazone derivatives.
- Band gap energy.
- Molecular electrostatic potential.

GRAPHICAL ABSTRACT

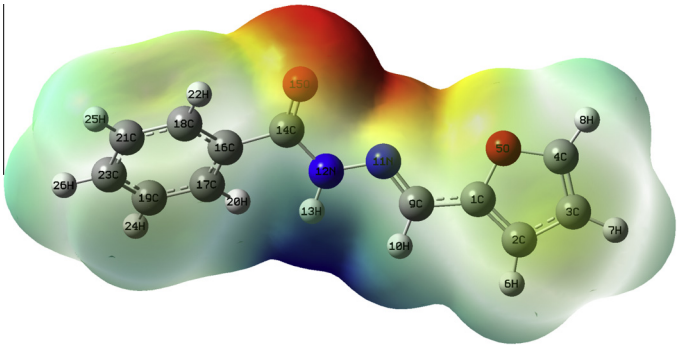

ARTICLE INFO

Article history:
Received 26 June 2013
Received in revised form 15 September 2013
Accepted 26 September 2013
Available online 8 October 2013

Keywords:
FT-IR
FT-Raman
TED
NBO
Furan
Hydrazone

ABSTRACT

The Spectral Characterization of *(E)-1-(Furan-2-yl) methylene)-2-(1-phenylvinyl) hydrazine* (FMPVH) were carried out by using FT-IR, FT-Raman and UV–Vis., Spectrometry. The B3LYP/6-311++G(d, p) level of optimization has been performed on the title compound. The conformational analysis was performed for this molecule, in which the *cis* and *trans* conformers were studied for spectral characterization. The recorded spectral results were compared with calculated results. The optimized bond parameters of FMPVH molecule was compared with X-ray diffraction data of related molecule. To study the intra-molecular charge transfers within the molecule the Lewis (bonding) and Non-Lewis (anti-bonding) structural calculation was performed. The Non-linear optical behavior of the title compound was measured using first order hyperpolarizability calculation. The atomic charges were calculated and analyzed.

Introduction

The hydrazones in the organic molecule brings several physical and chemical properties. Hydrazones are bearing the >C═N—N< leads the molecule towards nucleophilic and electrophilic nature. In hydrazone moiety the nitrogen atom behaves as nucleophilic and carbon atom behaves as nucleophilic as well as electrophilic nature [1–3]. The ability of hydrazones to react with both electrophilic and nucleophilic reagents widens their application in organic chemistry and designing the new drugs [1,4,5]. Several hydrazone derivatives have been reported as insecticides, nematocides, herbicides, rodenticides and antituburculosis in addition to that some of the hydrazone were found to be active against leukemia, sarcoma and illnesses [5,6]. Two types of photochemical reactions such as

* Corresponding author. Tel.: +91 9443879295.
E-mail addresses: nrbmiet@gmail.com (N. Ramesh Babu), saleem_h2001@yahoo.com (H. Saleem).

1386-1425/$ - see front matter © 2013 Elsevier B.V. All rights reserved.
http://dx.doi.org/10.1016/j.saa.2013.09.089

nitrogen–nitrogen bond cleavage and hydrogen migration from nitrogen to carbon were described for hydrazone [7,8]. The hydrazones were also shown to be involved in bio-molecular reactions such as cycloadditions and condensations [1,4]. In hydrazone containing C=N—N moiety, reveals existence of structural isomerism (E-entgegen 180° and Z-zusammen 0°), in which *E* conformer is most stable than *Z* conformer [9]. In the present investigations our main focus is to study the geometry of the molecule, vibrational behavior, non-linear optical activity and intra-molecular charge transfer analysis. For this we recorded FT-IR, FT-Raman and UV–Vis., spectra and also performed suitable theoretical calculation using B3LYP/6-311++G (d,p) level of basis set.

Experimental details

Synthesis

The 2.1 ml (0.025 mol) ethanolic solution of furan-2-aldehyde was added to (0.025 mol), 3.4 g of aqeous solution benzohydrazide taken in a R.B flask. The reaction mixture was kept over a magnetic stirrer and stirred well in an ice cold condition for an hour. The colorless solid separated out was filtered and dried over vacuum.

FT-IR, FT-Raman and UV–Vis., spectra

The FT-IR spectrum of FMPVH was recorded in the region 400–4000 cm^{-1} on an IFS 66 V spectrophotometer using the KBr pellet technique. The spectrum was recorded at room temperature with a scanning speed of 10 cm^{-1} per minute and at the spectral resolution of 2.0 cm^{-1} in SAIF Laboratory, IIT madras, Tamilnadu, India. The FT-Raman spectrum of title compound was recorded using the 1064 nm line of a Nd:YAG laser as excitation wavelength in the region 50–3500 cm^{-1} on Bruker model IFS 66 V spectrophotometer equipped with an FRA 106 FT-Raman module accessory and at spectral resolution of 4 cm^{-1}. The FT-Raman spectral measurements were carried out from SAIF Laboratory, IIT Madras, Tamilnadu, India. The ultraviolet absorption spectrum of FMPVH was recorded in the range of 200–500 nm using a Perkin Elmer Lambda-35 spectrometer, UV pattern is taken from a 10^{-5} molar solution of FMPVH dissolved in methanol.

Computational details

In order to establish the stable possible conformations, the conformational space of FMPVH compound was scanned with molecular mechanic simulations. For meeting the requirements of both accuracy and computing economy, theoretical methods and basis sets were considered. Density Functional Theory (DFT) has been proved to be extremely useful in treating electronic structure of molecules. The entire calculations were performed at B3LYP/6-311++G(d,p) level of basis set using Gaussian 03 W [10] program package, invoking gradient geometry optimization [10,11]. The optimized structural parameters were used in the vibrational frequency calculations at the DFT level to characterize all stationary points as minima. Then, vibrationaly averaged nuclear positions of FMPVH were used for harmonic vibrational frequency calculations resulting in IR and Raman frequencies together with intensities and Raman depolarization ratios. The vibrational modes were assigned on the basis of TED analysis using SQM program [12].

It should be noted that Gaussian 03 W package was able to calculate the Raman activities. The Raman activities were transformed into Raman intensities using Raint program [13] by the expression:

$$I_i = 10^{-12} \times (v_0 - v_i)^4 \times \frac{1}{v_i} \times \mathrm{RA}_i \quad (1)$$

where I_i is the Raman intensity, RA_i is the Raman scattering activities, v_i is the wavenumber of the normal modes and v_0 denotes the wavenumber of the excitation laser [14].

Results and discussion

Molecular geometry

The Optimization of FMPVH molecule was performed with B3LYP/6-311++G(d,p) level of basis set. The molecular geometry of FMPVH was well reproduced with X-ray diffraction data [15]. The optimized structure has shown in Fig. 1. In the present molecule due to the rotation of C_{14}—N_{12}—N_{11}—C_9 dihedral angle there seems a distortion in hydrazone linkage between phenyl and furan rings, rest of the bonds could not been disturbed. In FMPVH molecule the bond length of C_1—C_2, C_1—C_9 and C_2—C_3 are calculated 1.370, 1.445 and 1.425 Å. The experimental bond lengths of above are observed about 1.348, 1.432 and 1.415 Å [15]. The bond C_1—O_5 is appeared as σ bond character, its bond length is calculated about 1.364 Å. Similarly, the σ and π character of C_{14}=O_{15} bond is calculated about 1.212 Å. The experimental value of C_{14}=O_{15} bond is at 1.231 Å [15], which coincides well with calculated value. The σ and π bond characters of N_{12}-C_{14} and C_9—N_{11} are calculated as 1.390 and 1.282 Å are positively deviated with experimental (1.348 Å and 1.273 Å) data [15]. The deviation of bond length C_9—N_{11} is about 0.009 Å, it seems a good linearity with X-ray value [15]. The bond length of N_{11}—N_{12} is observed about 1.384 Å [15] which positively deviated (about 29 Å) from our theoretical value. The other calculated bond lengths in FMPVH were not much distorted in both conformers.

The bond angle of N_{12}—N_{11}—C_9 is calculated about 116.68°. Similarly, the bond angle of N_{11}—N_{12}—C_{14} is calculated as 121.31°, which nearly matches with experimental value of 119.16° [15]. From this investigation it fairly explores that, during the course of rotation of the bond, the entire molecule gets disturbed and the properties of the molecule also changes. From the literature [9] and our theoretical investigation, the optimized structure is more stable. The optimized bond parameters of FMPVH are listed in the Table 1.

Vibrational assignment

The vibrational analysis of FMPVH was studied on the basis of B3LYP/6-311++G (d,p) level of basis set. The vibrational assignments were carried out on the basis of furan, methylene, phenylvinyl and hydrazine group of this molecule. Furthermore, the molecule was predicted at local lowest minima on the potential energy surface and therefore none of the imaginary vibrational frequencies appeared. The title molecule is planar and belongs to C_1 point group. It consists of 26 atoms and hence it can have 72 normal modes of vibrations in which 25 stretching and 47 bending modes. To investigate the exact vibrational behavior of this molecule the total energy distribution (TED) analysis was performed on

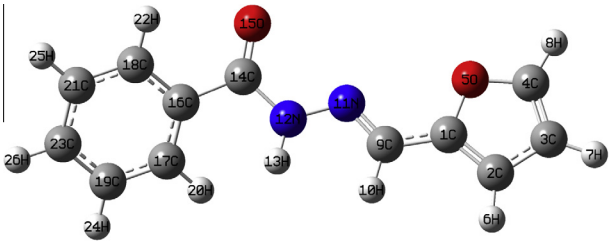

Fig. 1. The optimized molecular structure of FMPVH.

Table 1
The optimized bond parameters of FMPVH using B3LYP/6-311++G(d,p) level.

Parameters	Bond length (Å)	X-ray data[a]	Parameters	Bond angle (°)	X-ray data[a]
C1—C2	1.373	1.348	O5—C4—H8	115.76	124.5
C1—O5	1.364	1.366	C1—O5—C4	107.19	105.68
C1—C9	1.440	1.432	C1—C9—H10	114.86	119.10
C2—C3	1.427	1.415	C1—C9—N11	122.85	121.81
C2—H6	1.079	0.9300	H10—C9—N11	122.29	119.10
C3—C4	1.362	1.327	C9—N11—N12	116.68	115.43
C3—H7	1.078	0.9300	N11—N12—H13	119.40	120.40
C4—O5	1.358	1.368	N11—N12—C14	121.31	119.16
C4—H8	1.077	0.9300	H13—N12—C14	118.85	120.4
C9—H10	1.097	0.93	N12—C14—O15	123.36	122.65
C9—N11	1.282	1.273	N12—C14—C16	113.95	116.08
N11—N12	1.355	1.384	O15—C14—C16	122.68	121.24
N12—H13	1.016	0.860	C14—C16—C17	123.47	123.59
N12—C14	1.390	1.348	C14—C16—C18	117.29	117.59
C14—O15	1.212	1.2306	C17—C16—C18	119.21	118.82
C14—C16	1.504	1.490	C16—C17—C19	120.34	120.22
C16—C17	1.401	1.390	C16—C17—H20	120.59	119.9
C16—C18	1.400	1.387	C19—C17—H20	119.02	119.9
C17—C19	1.394	1.379	C16—C18—C21	120.37	120.39
C17—H20	1.085	0.930	C16—C18—H22	118.55	119.6
C18—C21	1.391	1.377	C21—C18—H22	121.08	119.6
C18—H22	1.083	0.9300	C17—C19—C23	120.07	120.23
C19—C23	1.393	1.380	C17—C19—H24	119.79	119.9
C19—H24	1.084	0.930	C23—C19—H24	120.14	119.9
C21—C23	1.395	1.376	C18—C21—C23	120.16	119.89
C21—H25	1.084	0.93	C18—C21—H25	119.80	119.6
C23—H26	1.084	0.93	C23—C21—H25	120.04	120.1
			C19—C23—C21	119.85	120.03
C2—C1—O5	109.66	110.11	C19—C23—H26	120.03	120.0
C2—C1—C9	130.48	130.51	C21—C23—H26	120.12	120.0
O5—C1—C9	119.86	119.36			
C1—C2—C3	106.47	106.54			
C1—C2—H6	126.10	126.70			
C3—C2—H6	127.42	126.7			
C2—C3—C4	105.94	106.65			
C2—C3—H7	127.58	126.70			
C4—C3—H7	126.48	126.7			
C3—C4—O5	110.74	111.01			
C3—C4—H8	133.50	124.5			

[a] Ref. [15].

the gas phase. The calculated wavenumbers were compared with recorded vibrational frequencies of FT-IR and FT-Raman spectra. Some discrepancies could be identified in between real and gas phase molecule and which were scaled down by proper scale factor [16]. The complete vibrational assignments along with the frequencies are presented in Table 2. The both recorded and theoretical spectra are shown in Figs. 2 and 3.

C—H Vibrations

The heteroaromatic molecule shows the presence of C—H stretching mode in the region 3100–3000 cm^{-1} which is the characteristic region for the ready identification of C—H stretching [17,18]. In this molecule nine C—H stretching vibrations are expected to occur, in which five from phenyl ring, three from furan ring and one from hydrazone linkage. The phenyl ring C—H stretching vibrations observed at 3060 (medium: m), 2923 (weak: w) and 3064 cm^{-1} (w) in FT-IR and FT-Raman spectra respectively. The calculated wavenumbers for the same mode lies at 3075, 3065, 3055, 3038 and 2908 cm^{-1} (mode numbers (mode Nos.) 5–7, 9 and 10). The harmonic C—H stretching modes corresponding to furan ring are assigned to 3151 (FT-IR: 3141w), 3126 and 3114 cm^{-1} (mode Nos. 2–4). The mode number 8 (3045 cm^{-1}) belongs to C—H stretching in hydrazone linkage. These assignments are in agreement with literature [17–19]. In aromatic compounds the C—H in-plane bending frequencies appear in the range 1000–1300 cm^{-1} and C—H out-of-plane bending appear in the range 750–1000 cm^{-1} [20,21]. In the present work, the in-plane pending vibration of δ_{CCH} is recorded at 1392 cm^{-1} (w), 1150 and 1014 cm^{-1} (m) in FT-IR spectrum and their Raman counterpart observed at 1393 and 1291 cm^{-1} as a medium strong band. On comparing these recorded values with theoretical values, the mode numbers 19, 22 and 27 are agreeable. The bands observed at 937, 896 (FT-IR) and 951, 790 cm^{-1} (FT-Raman) are assigned to C—H out-of-plane bending in FMPVH. The computed wavenumbers for the same mode observed at 953, 924, 904 and 786 cm^{-1} (mode Nos. 38, 39, 41 and 46). The observed and computed values for both C—H in-plane and out-of-plane modes show good linearity with one and other and also find support from literature [22].

N—H Vibrations

The stronger hydrogen band (HB) causes an increase of intensity, bandwidth and their wave number shift to lower value for the stretching vibration and higher wavenumbers for bending vibration [23]. In the present study the frequency of the vibrational mode of amine group (N—H) appears as pure and strong at 3246 cm^{-1} in FT-IR spectrum, while the computed wavenumber for this mode is 3362 cm^{-1} (mode No. 1). As per the investigation of Lorenc et al. [24] the N—H stretching mode appeared at 3262 (IR) and 3247 (Raman) cm^{-1}. When comparing our investigation with Lorenc et al. [25], the lowering of experimental frequency may be due to inter-molecular HB in the solid phase. The calculated TED values for this mode showed 100% pure as mentioned above. In-plane bending vibration of N—H mode is assigned at 1476 and 1477 cm^{-1} (medium strong) in FT-IR and FT-Raman

Table 2
The experimental and calculated frequencies of FMPVH using B3LYP/6-311++G(d,p) level of basis set (harmonic frequency (cm^{-1}), IR, Raman intensities (km/mol), reduced masses (amu) and force constants ($mdynA^{-1}$)).

Sl. no.	Frequencies		Observed		Intensity		Red. mass	Force const.	Vibrational assignments TED ⩾ 10%[d]
	Unscaled	Scaled[a]	FT-IR	FT-Raman	IR[b]	Raman[c]			
1	3499	3362	3246s		1.18	1.44	1.08	7.76	$\nu_{N12H13(100)}$,
2	3279	3151	3141w		0.04	0.85	1.11	7	$\nu_{C3H7(13)}$, $\nu_{C4H8\ (84)}$,
3	3253	3126			0.15	0.57	1.1	6.84	$\nu_{C2H6(87)}$,
4	3241	3114			1.18	0.54	1.09	6.76	$\nu_{C3H7(81)}$,
5	3200	3075			1.69	0.88	1.09	6.61	$\nu_{C18H22(81)}$, $\nu_{C21H25(14)}$,
6	3190	3065	3060m	3064w	3.45	1.22	1.1	6.57	$\nu_{C19H24(38)}$, $\nu_{C23H26(39)}$,
7	3180	3055			4.45	0.46	1.09	6.5	$\nu_{C17H20(13)}$, $\nu_{C19H24(33)}$, $\nu_{C21H25(38)}$, $\nu_{C23H26(11)}$,
8	3170	3045			0.72	0.54	1.09	6.44	$\nu_{C9H10(100)}$,
9	3162	3038			1.46	0.16	1.09	6.4	$\nu_{C17H20(27)}$, $\nu_{C21H25(36)}$, $\nu_{C23H26(34)}$,
10	3026	2908	2923w		10	0.38	1.09	5.86	$\nu_{C17H20(54)}$, $\nu_{C19H24(28)}$, $\nu_{C23H26(13)}$,
11	1761	1692	1646vs		80.6	4.86	11.11	20.31	$\nu_{C14=O15(74)}$,
12	1680	1614	1616s	1618vs	5.53	100	6.98	11.6	$\nu_{C9=N11(59)}$,
13	1640	1576	1569ms	1563ms	0.84	10.85	5.52	8.75	$\nu_{C19C17(19)}$, $\nu_{C21C18(21)}$,
14	1619	1555			1.13	0.37	5.52	8.51	$\nu_{C17C16(15)}$, $\nu_{C18C16(14)}$, $\nu_{C23C19(19)}$, $\nu_{C23C21(19)}$,
15	1598	1535	1540s		12.3	2.29	5.08	7.64	$\nu_{C2C1(38)}$, $\nu_{C4C3(14)}$, $\nu_{C9C1(17)}$,
16	1549	1488	1476m	1477ms	81.7	5.9	1.97	2.78	$\delta_{H13N12N11(29)}$, $\delta_{H13N12C14(24)}$,
17	1521	1462			3.31	2.17	2.24	3.06	$\nu_{CC(18)}$, $\delta_{CCH(17)}$, $\delta_{HCC(27)}$
18	1501	1442			12.6	22.95	3.52	4.67	$\nu_{C2C1(12)}$, $\nu_{C4C3(40)}$, $\nu_{O5C4H8(12)}$,
19	1475	1417	1392w	1393m	0.66	0.14	2.17	2.78	$\nu_{C19C17(10)}$, $\nu_{C21C18(10)}$, $\delta_{H26C23C19(14)}$, $\delta_{H26C23C21(14)}$,
20	1424	1368	1337ms	1338w	0.57	10.76	2.88	3.44	$\nu_{C3C2(16)}$, $\nu_{C4C3H7(12)}$, $\delta_{H8C4C3(12)}$,
21	1360	1307			3.85	6.61	1.5	1.64	$\nu_{C3C2(14)}$, $\delta_{H10C9C1(16)}$, $\delta_{H10C9N11(23)}$,
22	1352	1299		1291ms	0.42	0.31	1.69	1.81	$\delta_{H20C17C16(16)}$, $\delta_{C19C17H20(14)}$, $\delta_{H22C18C16(14)}$, $\delta_{C21C18H22(11)}$,
23	1332	1280	1288s	1276m	0.26	0.19	3.45	3.6	$\nu_{C17C16(20)}$, $\nu_{C18C16(20)}$,
24	1302	1251		1223	4.14	2.06	3.8	3.8	$\nu_{C14N12(15)}$, $\nu_{C16C14(16)}$,
25	1252	1203			100	26.72	3.19	2.95	$\nu_{C16C14(11)}$, $\delta_{H6C2C1(12)}$, $\delta_{C3C2H6(11)}$,
26	1242	1193			0.15	1.4	1.61	1.46	$\nu_{O5C1(28)}$, $\delta_{H10C9N11(12)}$,
27	1203	1155	1150m	1151w	8.4	1.86	1.15	0.98	$\nu_{C19C17(11)}$, $\delta_{H24C19C17(12)}$, $\delta_{C23C19H24(13)}$,
28	1184	1138			0.11	0.21	1.12	0.92	$\nu_{O5C4(22)}$, $_{O5C4H8(12)}$,
29	1182	1136			7.29	2.95	2.14	1.76	$\delta_{C23C21H25(10)}$, $\delta_{H26C23C19(17)}$, $\delta_{H26C23C21(15)}$,
30	1162	1116			55	12.14	3.65	2.9	$\nu_{N12N11(11)}$, $\delta_{C14N12(14)}$,
31	1108	1065	1078w		4.03	0.95	2.12	1.53	$\nu_{C3C2(11)}$, $\nu_{C4C3(12)}$, $\nu_{C4O5(37)}$,
32	1104	1061		1057w	2.69	1.39	2.02	1.45	$\nu_{C19C17(15)}$, $\nu_{C21C18(14)}$,
33	1074	1032			1.37	2.39	3.34	2.27	$\nu_{C23C19(22)}$, $\nu_{C23C21(20)}$,
34	1047	1006	1014m	1001w	3.91	2.42	2.36	1.53	$\nu_{C3C2(22)}$, $\delta_{C3C2H6(16)}$, $\delta_{C3C2H7\ (13)}$, $\delta_{C4C3H7(11)}$,
35	1037	996			6.58	3.63	1.38	0.87	$\delta_{CCC(35)}$
36	1016	976			0.82	4.58	5.81	3.53	$\nu_{N12N11(15)}$, $\nu_{C18C16(10)}$,
37	1010	970			0.17	0.04	1.32	0.8	$\Gamma_{H25C21C18H22(22)}$, $\Gamma_{H26C23C19H24(13)}$, $\Gamma_{H26C23C21H25(26)}$,
38	992	953		951w	0.36	0.08	1.37	0.79	$\Gamma_{H24C19C17H20(21)}$, $\Gamma_{H25C21C18H22(13)}$, $\Gamma_{H26C23C19H24(18)}$,
39	961	924	937m		10.8	1.16	3.51	1.91	$\Gamma_{H10C9C1C2(11)}$, $\Gamma_{H10C9C1O5(16)}$, $\Gamma_{N12N11C9H10(34)}$,
40	942	905			1.52	0.19	1.44	0.75	$\nu_{O5C1(12)}$, $\Gamma_{N12N11C9H10(16)}$,
41	941	904	896w		1.89	0.47	1.49	0.78	$\Gamma_{H24C19C17H20(15)}$,
42	915	879		883w	5.27	0.18	6.46	3.19	$\delta_{C14N12N11(11)}$, $\delta_{O15C14N12(13)}$,
43	903	868			2.37	1.19	6.13	2.95	$\delta_{C4C3C2(22)}$, $\delta_{O5C4C3(23)}$, $\delta_{H7C3C2(10)}$,
44	882	848			0	0.18	1.33	0.61	$\Gamma_{H7C3C2H6(38)}$, $\Gamma_{H8C4C3H7(24)}$,
45	860	826			0.32	0.23	1.25	0.54	$\Gamma_{C19C23C21H25(10)}$,
46	818	786		790w	2.14	0.08	1.34	0.53	$\Gamma_{C4C3C2H6(17)}$, $\Gamma_{H6C2C1O5(13)}$, $\Gamma_{H8C4C3H7(23)}$, $\Gamma_{H6C2C1C9(19)}$,
47	807	775			1.48	2.41	3.01	1.15	$\Gamma_{C17C16C14N12(10)}$, $\Gamma_{C18C16C14O15(12)}$,
48	793	762	763ms		4.23	0.74	4.6	1.71	$\delta_{N12N11C9(11)}$,
49	754	725			17.5	0.23	1.27	0.43	$\Gamma_{H7C3C2C1(13)}$, $\Gamma_{O5C4C3H7(19)}$, $\Gamma_{H8C4C3C2(30)}$, $\Gamma_{C1O5C4H8(15)}$,
50	718	690	690m		16.5	0.3	1.72	0.52	$\Gamma_{O15C14N12H13(11)}$,
51	704	676			1.84	0.05	3.11	0.91	$\Gamma_{CCCC(51)}$, $\Gamma_{HCCC(22)}$
52	693	666			5.77	0.3	6.38	1.8	$\delta_{C19C23C21(16)}$,
53	682	655	638m		0.18	0.12	4.88	1.34	$\Gamma_{C3C2C1O5(16)}$, $\Gamma_{C4O5C1C2(16)}$,
54	632	608	600w		0.26	0.73	6.3	1.48	$\delta_{C19C17C16(13)}$, $\delta_{C21C18C16(13)}$, $\delta_{C23C19C17(15)}$, $\delta_{C23C21C18(15)}$,
55	604	581			2.25	0.04	2.95	0.63	$\Gamma_{C4C3C2C1(16)}$, $\Gamma_{C1O5C4C3(18)}$, $\Gamma_{O5C4C3C2(26)}$,
56	547	525	535w		4.67	1.32	3.8	0.67	$\Gamma_{H13N12N11C9(33)}$, $\Gamma_{O15C14N12H13(20)}$, $\Gamma_{C16C14N12H13(34)}$,
57	521	500			11.2	1.18	1.29	0.21	$\delta_{C16C14N12(12)}$, $\delta_{O15C14C16(20)}$,
58	489	469			0.17	0.5	5.34	0.75	$\nu_{C9C1(11)}$,
59	421	404			2.36	0.54	4.62	0.48	$\delta_{C2C1C9(15)}$, $\delta_{O5C1C9(15)}$, $\delta_{N12N11C9(20)}$,
60	414	398			0.04	0.1	2.94	0.3	$\delta_{CCC(11)}$, $\Gamma_{CCCC(20)}$
61	387	372			0.53	0.15	7.67	0.68	$\Gamma_{C23C19C17C16(12)}$, $\Gamma_{C23C21C18C16(12)}$,
62	369	354			0.17	0.25	6.18	0.49	$_{N12N11C9C1(28)}$,
63	275	264		269w	2.75	0.32	3.91	0.17	$\delta_{O15C14N12(16)}$, $\delta_{C18C16C14(21)}$,
64	258	248			0.13	0.91	6.27	0.25	$\Gamma_{C3C2C1C9(12)}$, $\Gamma_{H10C9C1C2(15)}$, $\Gamma_{C14N12N11C9(11)}$,
65	237	228		192w	3.44	0.87	4.39	0.15	$\delta_{N12N11C9(11)}$,
66	181	174		162w	1.09	1.1	5.37	0.1	$\delta_{C14N12N11(14)}$,
67	133	127			0.41	0.89	5.92	0.06	$\delta_{C16C14N12(10)}$,
68	119	114		119w	0.85	1.18	6.12	0.05	$\Gamma_{C3C2C1C9(11)}$, $\Gamma_{N11C9C1O5(31)}$,
69	70	67		79ms	0.27	3.97	6.18	0.02	$\Gamma_{N12N11C9(13)}$, $\Gamma_{C17C16C14N12(14)}$, $\Gamma_{C17C16C14O15(11)}$,

(*continued on next page*)

Table 2 (*continued*)

Sl. no.	Frequencies		Observed		Intensity		Red. mass	Force const.	Vibrational assignments TED ⩾ 10%[d]
	Unscaled	Scaled[a]	FT-IR	FT-Raman	IR[b]	Raman[c]			
70	51	49			0.28	3.2	5.71	0.01	$\Gamma_{C16C14N12(10)}$, $\Gamma_{C18C16C14N12(13)}$, $\Gamma_{C18C16C14O15(10)}$,
71	37	36			0.2	8.88	4.01	0.00	$\Gamma_{N11C9C1O5(12)}$, $\Gamma_{H13N12N11C9(15)}$, $\Gamma_{C16C14N12N11(15)}$,
72	33	32			0.21	3.48	5.54	0.00	$\Gamma_{C14N12N11C9(22)}$, $\Gamma_{C16C14N12N11(23)}$,

v: Stretching, δ: in-plane-bending, Γ: out-of-plane bending, vw: very weak, w: weak, m: medium, s: strong, vs: very strong.
[a] Scaling factor: 0.9608 [16].
[b] Relative IR absorption intensities normalized with highest peak absorption equal to 100.
[c] Relative Raman intensities calculated by Eq. (1) and normalized to 100.
[d] Total energy distribution calculated at B3LYP/6-311++G(d,p) level.

spectra respectively. Furthermore the theoretical value showed about 1488 cm^{-1} with 53% of TED value. The out-of-plane bending vibration of N—H modes lies at 937 (m) and 535(w) cm^{-1} by FT-IR as mixed modes and are supported by harmonic mode numbers 39, 40 and 56.

C=O, C—O Vibrations

The presence of carbonyl group in FMPVH reveals several molecular properties. Studying the carbonyl group, the electron density of this group increases with decreasing bond length and hence the vibrational frequency shifted to the lower range. In evidence with this, the carbonyl peak appeared at 1646 cm^{-1} as a strong band. On contrary the DFT result assigned at 1692 cm^{-1} (mode No. 11) as pure as 74% of TED contribution.

In-plane-bending of $\delta_{C=O}$ contributes as a mixed vibration of $\delta_{O15\text{-}C14\text{-}N12}$, (mode Nos. 42 and 63) and $\delta_{O15—C14—C16}$ (mode No. 57) at 879, 264 and 500 cm^{-1} respectively. While comparing this with the experimental values 883 and 269 cm^{-1} as a weak band in FT-Raman spectrum, the contribution of $\delta_{C=O}$ calculated about 49% of TED. Out-of-plane mode of this group is recorded at 690 and 535 cm^{-1} in FT-IR, whereas the calculated frequency (mode Nos. 50 and 56) contributes about 11% and 20% of TED respectively.

The frequency calculated for $\nu_{C1—O5}$ and $\nu_{C4—O5}$ lies at 1193, 905 (28%, 12%) and 1138, 1065 cm^{-1} (and 22%, 37%) respectively, their corresponding experimental value observed at 1078 cm^{-1} (FT-1R). This negative deviation may be due to the inter-molecule charge delocalization within the furan ring and the maximum energy delocalization takes part in the σ–σ^* transition. This mode is supported by considerable TED values. On the basis of in-plane (δ_{OCC}, $_{OCH}$) and out-of-plane Γ_{OCCC}, $_{OCCH}$, $_{COCH}$ bending the vibrational wavenumber assigned to mode numbers 18, 28, 43 and 39, 46,

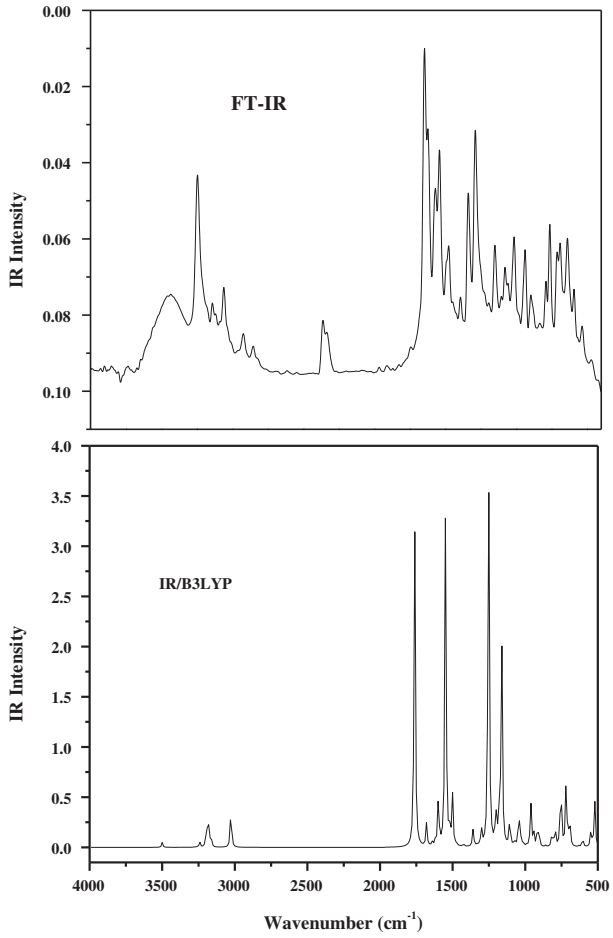

Fig. 2. The combined experimental and Theoretical IR spectrum of FMPVH.

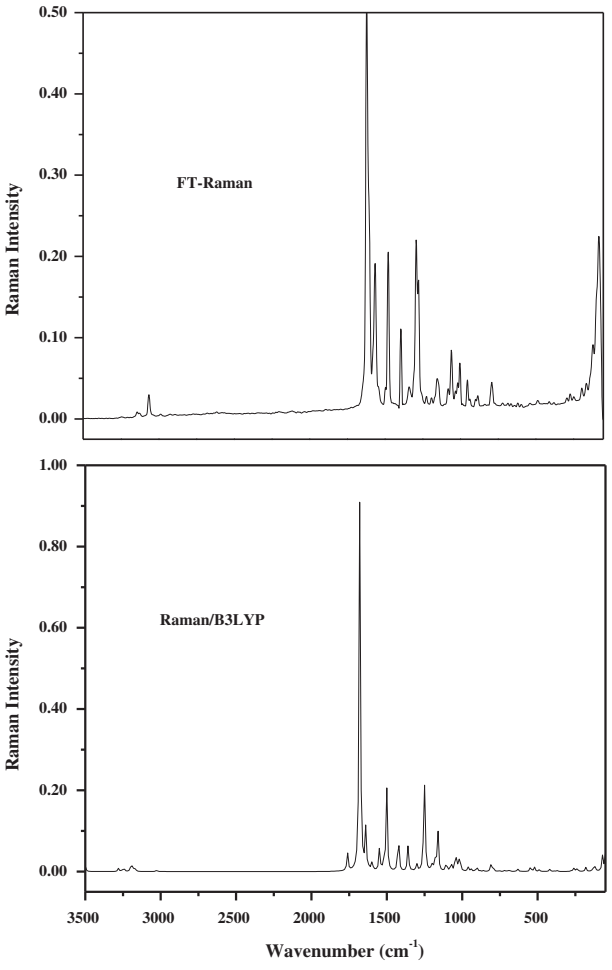

Fig. 3. The combined experimental and theoretical Raman spectrum of FMPVH.

49, 53, 55 respectively. While comparing these modes with experimental one, the mode number 53 shows a good agreement.

Diazo linkage group (—C═N—N—C—) vibrations

The hydrazone linkage fuses the phenyl and furan rings, which leads the vibrations as C═N, N—N and C—N as stretching as well as bending modes. The azo group stretching frequency undergoes a large down shift due to greater conjugation and π electron delocalization [26]. It is evident from our work, the bond length of π C_{9-} $=N_{11}$is lowered by decreasing electron density (ED)/1.923e and σ C_{14}—N_{12} is higher with increasing ED (1.989e) in the respective bond. Silverstein et al. [27], assigned the C—N stretching band at 1382–1266 $cm^{-1}$for aromatic amines. In an azo compound this mode expected in the region of 1200–1130 cm^{-1} [28,29]. Subramanian et al. [22] recorded a very intense Raman band at 1555 cm^{-1} originated from the stretching mode of C═N in the azo group. Our study predicted that the stretching of $\nu_{C9=N11}$ and $\nu_{C14-N12}$ groups were recorded as strong bands at 1616/1618 cm^{-1} (FT-IR/FT-Raman) and at1223 cm^{-1} (FT-Raman) respectively. Its theoretical values were predicted near to 1614 and 1251 cm^{-1} (mode Nos. 12, 24). The expected bending vibration of $\delta_{CNH,CCN}$ modes occurred at 1476 (FT-IR: m) and 1477 cm^{-1} (FT-Raman: m), their corresponding computed value at 1488 cm^{-1} (mode No. 16) with 24% of TED contribution. Similarly, the out-of-plane deformation was recorded and computed at 535 (w) and 525 cm^{-1} respectively, which abide good with reported literature value [22].

C═C, C—C Vibrations

The phenyl ring carbon–carbon stretching vibrations occur in the regions of 1625–1590 1590–1575, 1540–1470, 1465–1430 and 1380–1280 cm^{-1}were given by Varsanyi [30]. Carbon–carbon stretching bands of furan ring were recorded at 1553, 1531, 1555 and 1520 cm^{-1} for 2-furaldehyde dimethyl hydrazone [9]. In our present study, the carbon–carbon band observed at 1569 (m), 1392 (w), 1288 (strong: s) and 1150 (m) in FT-IR spectrum, on the other hand FT-Raman bands observed at 1563 (m), 1393 (m), 1276 (m) and 1151 (w) cm^{-1} for six membered ring. For six membered Skelekal $\nu_{C=C}$ and ν_{C-C} bands were predicted at 1576, 1555, 1417, 1280 and 1155 cm^{-1} by B3LYP/6-311++G (d,p) basis set. These computed wave numbers were calculated as mixed of π(C═C) and σ(C—C) bond character. Similarly, the furan ring C—C bands were assigned to 1540 (s), 1337 (m), 1078 (w) and 1014 (m) cm^{-1} in FT-IR and 1338 (w) in FT-Raman spectra. On comparing these values with computed frequencies, the mode numbers (15, 20, 21, 31 and 33) are in line with experimental values. These modes are mixed with C—H in-plane bending vibration in this region. The reported value of C—C bands [30] coincides well with observed, as well as computed values. The phenyl ring in-plane bending deformation was reported as a weak band at 1000 cm^{-1} [31]. Similar trend has been observed in the present case as observed at 1001 cm^{-1} in FT-Raman spectrum of FMPVH. The mode number 35 belongs to δ_{ccc} mode with 35% of TED.

The out-of-plane deformation of Γ_{CCCC} group is expected to occur in the range lower than δ_{CCC} group. The out-of-plane bending Γ_{CCCC} in furan ring appear as mixed vibrations of Γ_{CCCH}, $_{HCCC,OCCC}$ and Γ_{COCC} with considerable TED values. The observed frequencies 790 (FT-Raman), 638 (FT-IR) and 119 cm^{-1} (FT-Raman) are assigned to the same mode. Their corresponding theoretical wave numbers are 786, 655 and 114 cm^{-1}. Both the recorded and computed values are agreeable and also find support from literature [22].

Prediction of hyperpolarizability

The first order hyperpolarizabilities of FMPVH molecule is calculated using B3LYP/6-311++G(d,p) level of basis set, based on the finite-field approach. In the presence of an applied electric field, the energy of a system is a function of the electric field. First hyperpolarizability is a third rank tensor that can be described by a 3 × 3 × 3 matrix. The 27 components of the 3D matrix can be reduced to 10 components due to Kleinman symmetry [32]. It can be given in the lower tetrahedral format. It is obvious that the lower part of the 3 × 3 × 3 matrixes is a tetrahedral. The components of β are defined as the coefficients in the Taylor series expansion of the energy in the external electric field. When the external electric field is weak and homogeneous, this expansion becomes:

$$E = E^0 - \mu_\alpha F_\alpha - 1/2\alpha_{\alpha\beta}F_\alpha F_\beta - 1/6\beta_{\alpha\beta\gamma}F_\alpha F_\beta F_\gamma \quad (2)$$

where E^0 is the energy of the unperturbed molecules, F_α is the field at the origin, and $\mu_\alpha, \alpha_{\alpha\beta}, \beta_{\alpha\beta\gamma}$ is the components of the dipole moment, polarizability and the first order hyperpolarizabilities respectively. The total static dipole moment μ, the mean polarizability α_0, the anisotropy of polarizability Δα and the mean first hyperpolarizability β_0, using the *x*, *y*, *z* components are defined as

$$\mu = \left(\mu_x^2 + \mu_y^2 + \mu_z^2\right)^{1/2} \quad (3)$$

$$\alpha_0 = \frac{\alpha_{xx} + \alpha_{yy} + \alpha_{zz}}{3} \quad (4)$$

$$\Delta\alpha = 2^{-1/2}\left[\left(\alpha_{xx} - \alpha_{yy}\right)^2 + \left(\alpha_{yy} - \alpha_{zz}\right)^2 + \left(\alpha_{zz} - \alpha_{xx}\right)^2 + 6\left(\alpha_{xy}^2 + \alpha_{yz}^2 + \alpha_{xz}^2\right)\right]^{1/2} \quad (5)$$

$$\beta_0 = \left(\beta_x^2 + \beta_y^2 + \beta_z^2\right)^{1/2} \quad (6)$$

Many organic molecules, containing conjugated π electrons were characterized by large values of molecular first order hyper polarizabilities and analyzed by means of vibrational spectroscopy [33–36]. The intra-molecular charge transfer from the donor to acceptor group through a single-double bond conjugated path can induce large variations on both the molecular dipole moment and the molecular polarizability making IR and Raman activity strong at the same time [37].

The total molecular dipole moment (μ) and mean first order hyperpolarizability (β_0) are given as 1.0516 Debye and 17.866 × 10^{-30} esu, respectively. The total dipole moment of the title compound is approximately higher and the first order hyperpolarizability (β_0) of the title molecule is forty eight times greater

Table 3
The Non-linear measurements of FMPVH.

Parameters	Hyperpolarizability
β_{xxx}	−2048.67
β_{xxy}	479.46
β_{xyy}	−39.85
β_{yyy}	−56.77
β_{xxz}	87.45
β_{xyz}	−32.03
β_{yyz}	−7.20
β_{xzz}	60.29
β_{yzz}	−24.64
β_{zzz}	−13.73
β_0	17.866 × 10^{-30} esu
Parameters	Dipole moment
μ_x	−0.4860
μ_y	−0.9188
μ_z	−0.1872
μ	1.0561 Debye

Standard value for urea μ = 1.3732 Debye, β_0 = 0.3728 × 10^{-30} esu.

than that of the urea, hence this molecule has considerable NLO activity. The hyperpolarizabilities of FMPVH are given in Table 3.

Natural bond orbital (NBO) analysis

The hyperconjugation may be given as stabilizing effect that arises from an overlap between an occupied orbital with another neighboring electron deficient orbital, when these orbitals are properly oriented. This non-covalent bonding (antibonding) interaction can be quantitatively described in terms of the NBO analysis, which is expressed by means of the second-order perturbation interaction energy ($E^{(2)}$) [38–41]. This energy represents the estimate of the off-diagonal NBO Fock matrix elements. It can be deduced from the second-order perturbation approach [42].

$$E^{(2)} = \Delta E_{ij} = q_i \frac{F(i,j)^2}{\varepsilon_j - \varepsilon_i} \quad (7)$$

where q_i is the donor orbital occupancy, ε_i and ε_j are diagonal elements (orbital energies) and $F(i,j)$ is the off diagonal NBO Fock matrix elements. NBO analysis of FMPVH has been performed, in order to explain the intra-molecular charge transfer and delocalization of π-electrons. The intra-molecular hyperconjugative interaction is due to the overlap between π(C—C) and π*(C—C) the orbitals, which results in intra-molecular charge transfer, appeared in the molecular system [37].

In this present study, the NBO analysis has been carried out with B3LYP/6-311++G(d,p) level of basis set and which deals the intra-molecular charge transfer within the molecule. In any molecule, the π character of the bond plays an important role when compare with σ bond character. In such a way that this molecule delivers maximum delocalization energy during the transition between π and π* bond whereas the ED of the donor (Lewis) bond decreases with increasing of ED of acceptor (Non-Lewis) bonds. In accordance with the above, the title molecule shows 67.53 and 81.59 kJ/mol of energy during the interaction between $\pi C_1—C_2$ and $\pi^*C_3—C_4$, $\pi^*C_9—N_{11}$ bonds, on the other hand the $\sigma C_1—C_2$ and $\sigma^*C_1—C_9$ shows about 15.56 kJ/mol energy. The electron densities of the above bonds are about 1.982e ($\sigma C_1—C_2$) and 0.029e ($\sigma^*C_1—C_9$) for the donor and accepter bond respectively. The electron densities of $\pi C_1—C_2$ and $\pi^*C_3—C_4$ are calculated about 1.793e and 0.262e respectively. From these observations the σ–σ* and π–π* interaction reveals that, the ED of particular π bond decreases with increasing of π* ED and vice versa for σ and σ* bond which may be due to the delocalization. Similarly, the π and π* interaction in the molecule appear as the maximum delocalization energy which leads the molecule become highly active. The lone pair of oxygen and nitrogen atoms play great role in the molecule. The O_5 atom transfers 119.75 kJ/mol and 118.95 kJ/mol to $\pi^*C_1—C_2$ and $\pi^*C_3—C_4$ bonds respectively. In the same way the N_{12} transfers 122.17 kJ/mol to $\pi^*C_9—N_{11}$ and O_{15} transfers 120 kJ/mol to $\pi^*N_{12}—C_{14}$. The maximum hyperconjugative $E^{(2)}$ energy of heteroatoms during the intra-molecular interaction leads the molecule towards medicinal and biological applications. The lewis and non-lewis NBO's of the FMPVH are given in Table S1 (Supporting information).

HOMO–LUMO analysis

The highest occupied molecular orbital (HOMO) and Lowest unoccupied molecular orbital (LUMO) are the main orbitals that take part in chemical stability. The HOMO represents the ability to donate an electron, LUMO as an electron acceptor represents the ability to obtain an electron. This also predicted that the nature of electrophiles and nucleophiles to the atom where the HOMO and LUMO are stronger. The energy gap FMPVH was calculated using B3LYP/6-311++G(d,p) level. In this title compound, highest electronic energy lies at furan ring and hydrazone linkage and the HOMO is calculated about −6.093 eV. The kinetic energy of the 56th occupied level (HOMO) is calculated as 1.59 a.u. The lowest electronic energy appeared in the phenyl ring, which exhibited at 57th virtual orbital and measured as LUMO value −1.927 eV, along with kinetic energy of 1.618 a.u. The energy gap of HOMO and LUMO could be determined about −4.166 eV, which leads the molecule becomes less stability and more reactivity. Moreover,

Table 4
The Frontier molecular orbital of FMPVH.

Occupancy	Orbital energies a.u	Orbital energies in eV	Kinetic energies a.u
O_{52}	−0.289	−7.875	1.500
O_{53}	−0.278	−7.556	1.631
O_{54}	−0.274	−7.468	1.160
O_{55}	−0.262	−7.143	2.007
O_{56}	−0.224	−6.093	1.590
V_{57}	−0.071	−1.927	1.618
V_{58}	−0.042	−1.139	1.527
V_{59}	−0.031	−0.842	1.251
V_{60}	−0.020	−0.541	0.333
V_{61}	−0.007	−0.198	0.229

O – occupied level; V – virtual level.

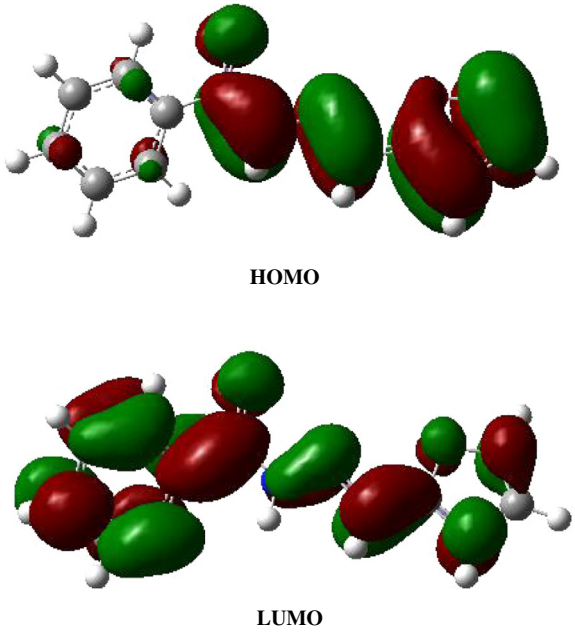

Fig. 4. The frontier molecular orbital of FMPVH.

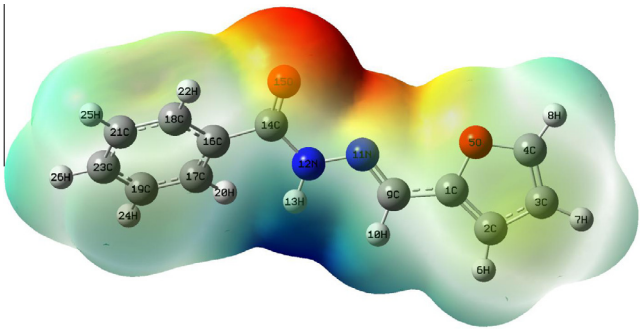

Fig. 5. Molecular electrostatic potential of FMPVH.

Table 5
The excitation energies and oscillator strengths of FMPVH.

Excited state 1	Singlet-A	Excitation energy		Observed energy	Oscillator strength
56 → 57	0.63164	3.8992 eV	317.98 nm	352.62	$f = 0.7366$
56 → 58	0.16574				
Excited state 2	Singlet-A				
53 → 57	−0.28316				
55 → 57	0.60525	4.2356 eV	292.72 nm	303.49	$f = 0.0139$
55 → 58	0.10827				
Excited state 3	Singlet-A				
56 → 58	0.61443	4.5733 eV	271.10 nm		$f = 0.2133$
56 → 59	0.21926				

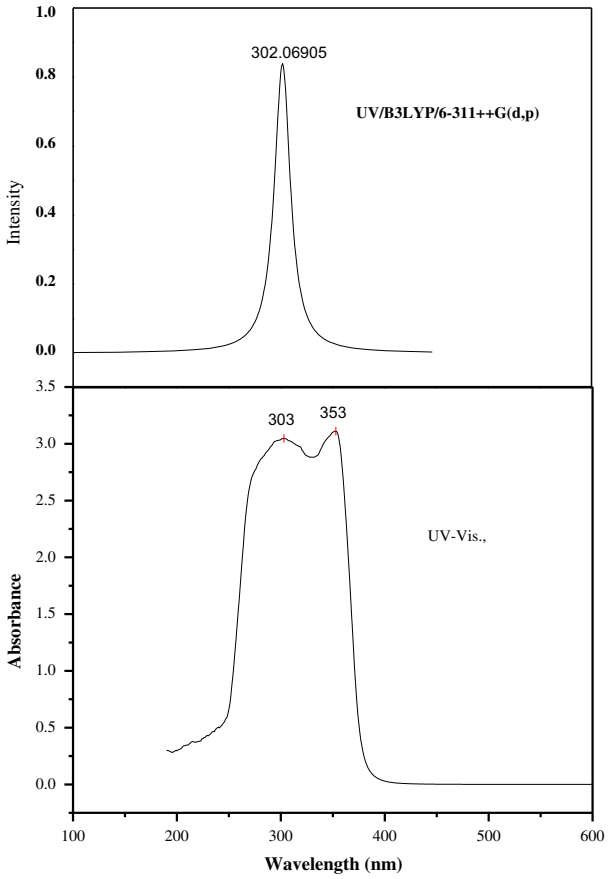

Fig. 6. The UV-spectrum of FMPVH.

the separation of Homo and Lumo determines that the molecule becomes active in any field. In such a way, the energy of occupied levels 55, 54, 53 and 52 were calculated about −7.143, −7.468, −7.556 and −7.875 eV whereas the unoccupied levels lies in the ranges at −1.927 (V_{57}) −1.139 (V_{58}), −0.842 (V_{59}), −0.541 (V_{60}) and −0.198 (V_{61}). The calculated energies of frontier molecular orbitals are listed in Table 4. Corresponding frontier molecular orbitals are shown in Fig. 4.

Electrostatic potential

The information provided by inspection of the Homo and Lumo is thus visualizing the electrostatic potential (ESP). The electrophiles tend to negative ESP and nucleophiles tend to region of positive ESP. In accord with this the carbonyl and furan ring behaves as electrophiles region and it is denoted as *exo* face (top) as red color. The molecular electrostatic potential was calculated with B3LYP/6-311++G(d, p) level of basis set. The calculated electrostatic energy is about −606.67 eV and −609.52 eV for O_5 and O_{15} respectively. Similarly, the nucleophiles region was graphically shown as in the *endo* face (bottom) region. It is possibly denoted by the blue color and expressed electron deficiency in those regions, which also denotes nucleonic energy of Lumo orbitals. The calculated nucleophiles energies are about −499.51 (N_{11}) and −498.67 eV for the hydrazone region. The ESP diagram is shown in Fig. 5 and calculated electrostatic energies are given in Table S2. The atomic charge plot of FMPVH is shown in Fig. S1 (Supporting information).

UV-analysis

The ultraviolet spectrum which results from the promotion of an electron in an occupied molecular orbital (MO) of ground electronic state molecule into a virtual MO, thus forming an electronically excited state [43]. The UV analysis was carried out using B3LYP/6-311++G(d, p) level of basis set for FMPVH. The recorded electronic spectrum of FMPVH shows the transitions at 352 nm and 302 nm, which clearly understands that the recorded region 352 nm relatively coincides with calculated value of 317 nm. The calculated results of FMPVH possess three excited states (ES), in which ES-1 appeared at 317.98 nm (3.899 eV), ES-2 at 292.72 nm and ES-3 lies at 271.10 nm. The ES-1 reveals the transition between $HOMO_{56}$ to $LUMO_{57}$ and also next level $LUMO_{58}$. And for ES-2 there are three transitions from $HOMO_{53}$–$LUMO_{57}$, $HOMO_{55}$–$LUMO_{57}$ and $LUMO_{58}$. In which the transition of electron from $HOMO_{53}$ to $LUMO_{57}$ is larger on comparing with other transitions. The calculated band gap (292.72 nm) of ES-2 coincides well with the recorded value of 303.49 nm. In the same way, ES-3 has two transition namely $HOMO_{56}$–$LUMO_{58}$ and $LUMO_{59}$ and their band gap energy is about 4.573 eV (271.10 nm). The excitation energies of FMPVH are listed in Table 5. The UV–Vis., spectrum of FMPVH has shown in Fig. 6.

Conclusion

The complete vibrational analysis has been performed for the first time to the FMPVH. The optimized geometrical parameters are agrees well with literature value. The observed FT-IR and FT-Raman spectral values are well supported by calculated values. The vibrational frequencies for C=O and C=N (functional groups) are shifted to lower frequency, which is due to the presence of π-bonds. The calculated first order hyperpolarizability of FMPVH molecule is found to be 17.866×10^{-30} esu, which is forty-eight times greater than that of urea. NBO result reflects the charge transfer within the molecule and the maximum charge delocalization takes place during π–π* transition. The band gap of FMPVH molecule was determined about −4.166 eV, which leads the molecule becomes less stability and more reactivity. The MEP

represents that the carbonyl group and furan ring behaves as electrophiles region and hydrozone region behaves as nucleophiles. The recorded UV–Vis., spectral values agree well with calculated values.

Appendix A. Supplementary material

Supplementary data associated with this article can be found, in the online version, at http://dx.doi.org/10.1016/j.saa.2013.09.089.

References

[1] N.P. Belskaya, W. Dehaen, V.A. Bakulev, Arkivoc (i) (2010) 275–332.
[2] S. Kim, J.-Y. Yoon, Sci. Synth. 27 (2004) 671–722.
[3] R. Brehme, D. Enders, R. Fernandez, J.M. Lassaletta, Eur. J. Org. Chem. 34 (2007) 5629–5660.
[4] S. Dadiboyena, A. Nefzi, Eur. J. Med. Chem. 46 (2011) 5257–5258.
[5] Y.P. Kitaev, B.I. Buzykin, T.V. Troepol'skaya, Russ. Chem. Rev. 39 (1970) 441–456.
[6] A.M. Wu, P.D. Senter, Nat. Biotechnol. 23 (2005) 1137–1146.
[7] R.W. Binkley, Tetahedron Lett. 23 (1969) 1893.
[8] S.D. Carson, J. Org. Chem. 35 (1970) 2734–2736.
[9] C. Araujo-Andrade, B.M. Giuliano, A. Gómez-Zavaglia, R. Fausto, Spectrochim. Acta A 97 (2012) 830–837.
[10] M.J. Frisch, G.W. Trucks, H.B. Schlegel, G.E. Scuseria, M.A. Robb, J.R. Cheeseman, J.A. Montgomery Jr., T. Vreven, K.N. Kudin, J.C. Burant, J.M. Millam, S.S. Iyengar, J. Tomasi, V. Barone, B. Mennucci, M. Cossi, G. Scalmani, N. Rega, G.A. Petersson, H. Nakatsuji, M. Hada, M. Ehara, K. Toyota, R. Fukuda, J. Hasegawa, M. Ishida, T. Nakajima, Y. Honda, O. Kitao, H. Nakai, M. Klene, X. Li, Knox, H.P. Hratchian, J.B. Cross, C. Adamo, J. Jaramillo, R. Gomperts, R.E. Stratmann, O. Yazyev, A.J. Austin, R. Cammi, C. Pomelli, J.W. Ochterski, P.Y. Ayala, K. Morokuma, G.A. Voth, P. Salvador, J.J. Dannenberg, V.G. Zakrzewski, S. Dapprich, A.D. Daniels, M.C. Strain, O. Farkas, D.K. Malick, A.D. Rabuck, K. Raghavachari, J.B. Foresman, J.V. Ortiz, Q. Cui, A.G. Baboul, S. Clifford, J. Cioslowski, B.B. Stefanov, G. Liu, A. Liashenko, P. Piskorz, I. Komaromi, R.L. Martin, D.J. Fox, T. Keith, M.A. Al-Laham, C.Y. Peng, A. Nanayakkara, M. Challacombe, P.M.W. Gill, B. Johnson, W. Chen, M.W. Wong, C. Gonzalez, J.A. Pople, Gaussian 03, Revision C.02, Gaussian Inc., Wallingford, CT, 2004.
[11] H.B. Schlegel, J. Comput. Chem. 3 (1982) 214–218.
[12] G. Rauhut, P. Pulay, J. Phys. Chem. 99 (1995) 3093–3100.
[13] D. Michalska, Raint Program, Wroclaw University of Technology, 2003.
[14] D. Michalska, R. Wysokinski, Chem. Phys. Lett. 403 (2005) 211–217.
[15] M.Z. Song, C.G. Fan, Acta Cryst. E 65 (2009) o2800.
[16] M.A. Palafox, Int. J. Quantum Chem. 77 (2000) 661–684.
[17] V.K. Rastogi, M.A. Palafox, R.P. Tanwar, L. Mittal, Spectrochim. Acta A 58 (2002) 1989.
[18] M. Silverstein, G.C. Basseler, C. Morill, Spectrometric Identification of Organic Compounds, Wiley, New York, 1981.
[19] T. Iliescu, F.D. Irimie, M. Bolboaca, Cs. Paisz, W. Kiefer, Vib. Spectrosc. 29 (2002) 235–239.
[20] G. Socrates, Infrared Characteristic Group Frequencies, Wiley, New York, 1980.
[21] G. Varsanyi, Vibrational Spectra of Benzene Derivatives, Academic Press, New York, 1969.
[22] N. Subramanian, N. Sundaraganesan, J. Jayabharathi, Spectrochim. Acta A 76 (2010) 259–269.
[23] G.C. Pimentel, A.L. McClellan, The Hydrogen Bond, Freeman and Comp., San Francisco, 1960. 176.
[24] J. Lorenc, Vib. Spectrosc. 61 (2012) 112–123.
[25] J. Lorenc, J. Hanuza, J. Janczak, Vib. Spectrosc. 59 (2012) 59–70.
[26] D.L. Vein, N.B. Colthup, W.G. Fateley, J.G. Grasselli, The Handbook of Infrared and Raman Characteristic Frequencies of Organic Molecules, Academic Press, New York, 1991.
[27] M. Silverstein, G. Clayton Basseler, C. Morill, Spectrometric Identification of Organic Compounds, Wiley, New York, 1981.
[28] P. Vandenabeele, L. Moens, H.G.M. Edwards, R. Dams, J. Raman Spectrosc. 31 (2000) 509.
[29] P.J. Trotter, Appl. Spectrosc. 31 (1977) 30–35.
[30] G. Varsanyi, Assignments of Vibrational Spectra of Seven Hundred Benzene Derivatives, vol. 1–2, Adam Hilger, 1974.
[31] N. Sundaraganesan, J. Karpagam, S. Sebastian, J.P. Cornard, Spectrochim. Acta A 73 (2009) 11–19.
[32] N.B. Colthup, L.H. Daly, S.E. Wiberly, Introduction to Infrared and Raman Spectroscopy, Academic Press, New York, 1990.
[33] C. Castiglioni, M. Del zoppo, P. Zuliani, G. Zerbi, Synth. Met. 74 (1995) 171–177.
[34] P. Zuliani, M. Del zoppo, C. Castiglioni, G. Zerbi, S.R. Marder, J.W. Perry, Chem. Phys. 103 (1995) 9935–9940.
[35] M. Del zoppo, C. Castiglioni, G. Zerbi, Non-Linear Opt. 9 (1995) 73.
[36] M. Del zoppo, C. Castiglioni, P. Zuliani, A. Razelli, G. Zerbi, M. Blanchard-Desce, J. Appl. Polym. Sci. 70 (1998) 73.
[37] C. Ravikumar, I. Huber Joe, V.S. Jayakumar, Chem. Phys. Lett. 460 (2008) 552–558.
[38] A.E. Reed, F. Weinhold, J. Chem. Phys. 78 (1983) 4066–4073.
[39] A.E. Reed, F. Weinhold, J. Chem. Phys. 83 (1985) 1736–1740.
[40] A.E. Reed, R.B. Weinstock, F. Weinhold, J. Chem. Phys. 83 (1985) 735–746.
[41] J.P. Foster, F. Wienhold, J. Am. Chem. Soc. 102 (1980) 7211–7218.
[42] J. Chocholousova, V. Vladimir Spirko, P. Hobza, Phys. Chem. Chem. Phys. 6 (2004) 37–41.
[43] R. M Silverstein, F.X. Webster, Spectrometric Identification of Organic Compounds, sixth ed., Wiley, New York, 1997.